Available online at www.sciencedirect.com
ScienceDirect
Bioorganic & Medicinal Chemistry 15 (2007) 4577–4584
Bioorganic & Medicinal Chemistry

Isolation of new phenylacetylingol derivatives that reactivate HIV-1 latency and a novel spirotriterpenoid from *Euphorbia officinarum* latex

Mourad Daoubi,[a] Nieves Marquez,[c] Noureddine Mazoir,[b] Ahmed Benharref,[b] Rosario Hernández-Galán,[a] Eduardo Muñoz[c] and Isidro G. Collado[a,*]

[a]*Departamento de Química Orgánica, Facultad de Ciencias, Universidad de Cádiz, Apdo. 40, 11510 Puerto Real, Cádiz, Spain*
[b]*Laboratoire de Chimie des Substances Naturelles, Faculté des Sciences Semlalia, Université Cadi Ayyad, Marrakech, Morocco*
[c]*Departamento de Biología Celular, Fisiología e Inmunología, Facultad de Medicina, Universidad de Córdoba, Avda de Menendez Pidal s/n, 14004 Córdoba, Spain*

Received 20 November 2006; revised 22 March 2007; accepted 5 April 2007
Available online 10 April 2007

Abstract—Three new, highly functionalized ingol diterpenes, ingol 7,8,12-triacetate 3-phenylacetate (**1**), ingol 7,8,12-triacetate 3-(4-methoxyphenyl)acetate (**2**) and 8-methoxyingol 7,12-diacetate 3-phenylacetate (**3**), together with the novel spirotriterpene, 3*S*,4*S*,5*R*,7*S*,9*R*,14*R*-3,7-dihydroxy-4,14-dimethyl-7[8 → 9]-*Abeo*-cholestan-8-one (**4**), have been isolated from *Euphorbia officinarum* latex. Structures were established on the basis of their spectroscopic data, including two-dimensional NMR analysis and NOE experiments. The biological effects of **1**–**3** on cell cycle and HIV-1 gene transcription were analysed in the Jurkat T cell line. Compound **3** induced cell-cycle arrest and HIV-1-LTR promoter activation and could represent a novel lead compound for the development of therapies against HIV-1 latency.

1. Introduction

The *Euphorbia* genus comprises a large and diverse group of plants which are characterized by the presence of a milky white latex. Due to its potential medical applications, this genus has been the subject of abundant phytochemical and pharmacological research. Indeed, extracts of numerous species have been found to demonstrate a number of interesting biological activities against leukaemia in mice and pathologies such as cancer, swelling and warts.[1–6] Our own research has focused on *Euphorbia officinarum*, which is used in traditional medicine to treat skin and ophthalmologic diseases. It should be noted that due to its high toxicity, the plant extract must always be used in low concentrations. [1–6] Nevertheless, many biologically active natural compounds have been isolated from this genus.[7] For instance, phorbol and ingenol derivatives have been identified as potent anti-proliferative compounds in tumour cells.[8–10] Moreover, some deoxyphorbols such prostratin (12-deoxyphorbol 13-acetate) have received a lot of attention recently because of their potential use against AIDS.[11] Prostratin, as well as other deoxyphorbols, prevents chemically induced skin carcinogenesis and induces HIV-1 reactivation in virally infected latent cells.[12,13] HIV-1 latency is one of the major barriers preventing eradication of the virus from the infected body. The virus remains in a relatively latent state in a small but clinically important fraction of $CD4^+$ memory T cells which contain integrated but transcriptionally inactive proviruses.[14] Hence, the rebound viremia typically observed in patients coming off of effective ART (anti-retroviral therapy) probably involves viral reseeding from this latent reservoir and therefore new approaches to the elimination of these latently infected cells are urgently needed.

This paper reports on the isolation, structure determination and biological activities of three new ingol diterpenes (**1**–**3**). We found that compound **3** induced cell-cycle arrest and HIV-1 gene reactivation in the leukaemia cell line Jurkat-LTR-GFP, representing a valid model for the investigation of HIV-1 latency.

Keywords: *Euphorbia officinarum*; Euphorbiaceae; Diterpenoids; Ingol esters; Spiro-triterpenoids; Cell cycle; HIV-1 latency.
* Corresponding author. Tel.: +34 956 016368; fax: +34 956 016193; e-mail: isidro.gonzalez@uca.es

0968-0896/$ - see front matter © 2007 Elsevier Ltd. All rights reserved.
doi:10.1016/j.bmc.2007.04.009

2. Results and discussion

Within the context of our search for the chemical constituents of *E. officinarum*, we isolated three components structurally related to the ingol skeleton (**1**–**3**) and a novel spirotriterpene (**4**). The structures of these three compounds and that of the spirotriterpene (**4**), including their stereochemical aspects, were determined by means of mass spectrometry and extensive 1D and 2D NMR (COSY, HMQC, HMBC and NOESY) and X-ray analysis.

The hydrogen and carbon connectivities deduced from HMQC and HMBC experiments aided in establishing the structure of macrocyclic lathyrane-type diterpenoids, allowing us to conclude that compounds **1**–**3** are structurally close to a tri- or tetraester of ingol-bearing various types of acyl groups. Ingol are macrocyclic diterpenes based on the parent hydrocarbon lathyrane, and are biogenetically related to the compounds of the tigliane, daphnane and ingenane types.[15] Comparison of the spectroscopic data corresponding to compounds **1**–**3** with those described for esters of ingol,[16–20] showed a relevant difference in the chemical shift of the H-5 protons, which appear in the spectra of ingol derivatives reported in the literature at δ 5.60–5.80, a marked difference with compounds **1**–**3** (Table 1), where it appears at δ 5.32–5.39 ppm. The similarity in the chemical shift and coupling constant values corresponding to the rest of the protons with those published for essentially the same in all of these compounds.[16,17,21] NOE and NOESY correlations observed in all cases confirmed this to be true. Hence, NOE interaction (Fig. 1a) was visible between the H-3 and H-5. H-5 gave further interactions with H-9. Further NOEs were observed between H-8 and both H-7 and H-12. On the other hand, the values of J_{2-3}(≈8.5 Hz) and the chemical shifts of H-1 protons, indicate that the configuration at C-2 and C-3 is 2 *S*, 3*S*, as in true ingol derivatives.[21] It can therefore be assumed that **1**–**3** have the same absolute configuration as other ingol derivatives.[22] Based on this, we considered all possible positional isomers of ingol triacetate phenylacetate, optimized their geometry and got the lowest energy conformers for each possible diastereoisomer.[23] For three of them, those where phenylacetoxy group was bound on 11-membered ring carbons: C-7, C-8 or C-12; vinylic proton H-5 was lined with the carbonyl group on C-14, as shown by the dotted circles in Figure 1b, while for the 3-phenylacetoxy derivative the preferred conformation places both groups in anti disposition (Fig. 1a). From this we concluded that compounds **1**–**3** are ingol derivatives bearing phenylacetoxy or methoxyphenylacetoxy groups at C-3 (Scheme 1).

Compounds **1** and **2** showed very similar ^{1}H and ^{13}C NMR, with the exception of signals from benzylacetyl esters. Compound **1**'s molecular formula was established as $C_{34}H_{42}O_{10}$ on the basis of HREIMS data (*m*/*z* 610.2800 $[M]^+$). The EI mass spectrum displayed the prominent peak at *m*/*z* = 91 $[C_7H_7]^+$ and fragments due to the sequential loss of Ac, AcOH and $C_6H_5CH_2CO_2H$, indicating the presence of three acetyl groups and one phenylacetyl group. Compound **2**, however, gave a molecular ion at *m*/*z* = 640.2874, indicating

Table 1. ^{1}H NMR[a] data of compounds **1**–**3** (600 MHz, δ [ppm])

H	**1** δ (mult, *J*/Hz)	**2** δ (mult, *J*/Hz)	**3** δ (mult, *J*/Hz)
1α	2.76 (dd, 9.0, 15.0)	2.76 (dd, 9.0, 15.0)	2.75 (dd, 9.0, 14.8)
1β	1.67 (d, 15.0)	1.66 (d, 15.0)	1.65 (d, 14.8)
2	2.5 (m)	2.49 (m)	2.47 (m)
3	5.14 (d, 8.6)	5.14 (d, 8.6)	5.1 (d, 8.6)
4	—	—	—
5	5.38 (br s)	5.39 (br s)	5.32 (br s)
6	—	—	—
7	5.14 (d, 1.9)	5.12 (d, 1.9)	5.22 (br s)
8	4.52 (dd, 1.9, 10.7)	4.52 (dd, 1.9, 10.7)	2.87 (dd, 1.9, 10.1)
9	1.09 (dd, 9.0, 10.9)	1.11 (dd, 9.1, 10.7)	1.06 (superimposed signal)
10	—	—	—
11	1.02 (dd, 9.0, 10.9)	1.02 (superimposed signal)	0.94 (superimposed signal)
12	4.81 (dd, 3.4, 10.9)	4.82 (dd, 3.8, 11.0)	4.82 (dd, 3.8, 10.9)
13	2.86 (qd, 3.8, 7.1)	2.87 (qd, 3.8, 7.3)	2.86 (qd, 4.1, 7.0)
14	—	—	—
15	—	—	—
16	0.91 (d, 7.5)	0.91 (d, 7.5)	0.91 (d, 7.5)
17	2.06 (d, 1.2)	2.06 (d, 1.2)	1.99 (br s)
18	1.04 (s)	1.04 (s)	1.06 (s)
19	0.81 (s)	0.81 (s)	0.95 (s)
20	1.04 (d, 7.1)	1.04 (superimposed signal)	1.02 (d, 7.3)
OAc	1.95 (s), 2.05 (s)	1.96 (s), 2.05 (s)	2.1 (s), 2.03 (s)
R_1	3.70 (br s) (CH_2)	3.79 (s) (Ome)	3.71 (d, 15.6)
	7.25 (m)	3.64 (br s) (CH_2)	3.69 (d, 15.6)
	7.28 (m)	7.18, 8.8	7.25 (m)
		6.84 (d, 8.8)	7.29 (m)
R_2	2.08 (s)	2.08 (s)	3.28 (s)

[a] Recorded in $CDCl_3$ (δ_H 7.25).

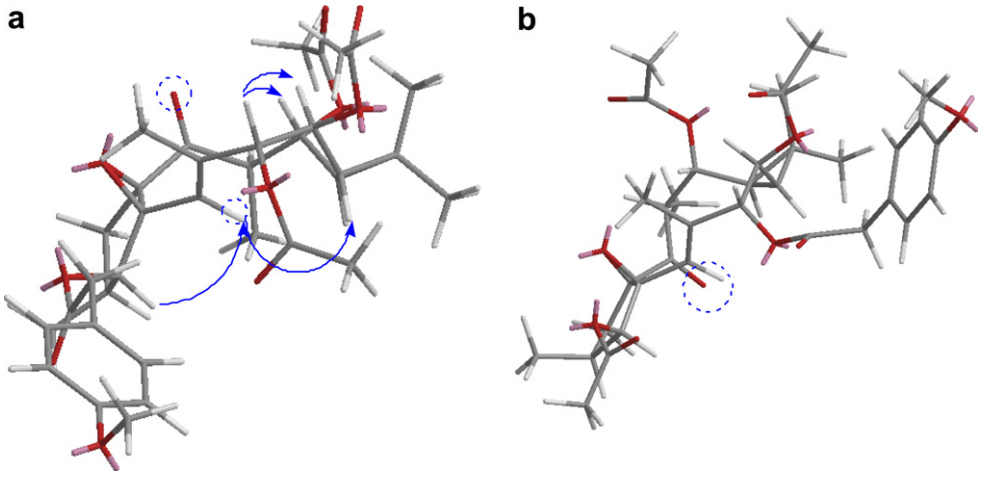

Figure 1. Calculated conformation of compound **2** (a) and ingol 3,8,12-triacetate 7-(*p*-methoxyphenyl)acetate (b).

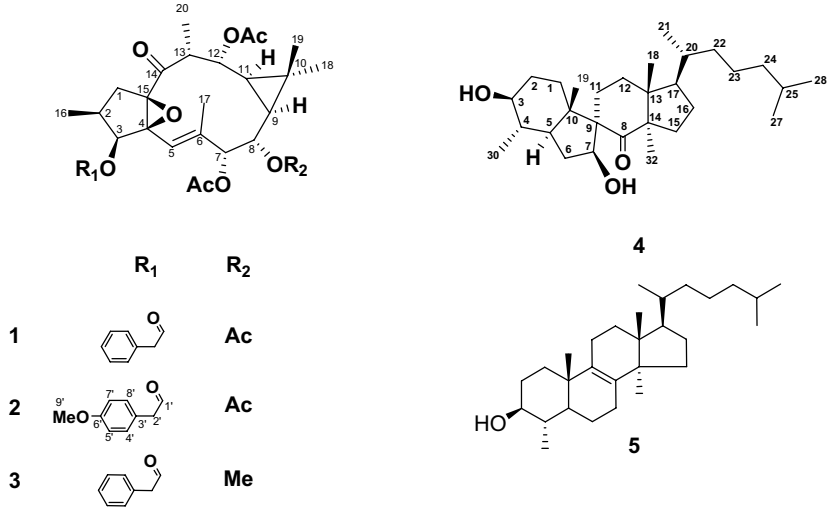

Scheme 1. Isolated compounds from *E. officinarum*.

a molecular formula of $C_{35}H_{44}O_{11}$. Fragments *m/z* = 121 $[C_8H_9O]^+$ (base peak) and *m/z* = 148 $[C_9H_8O]^+$ indicate the presence of a *p*-methoxyphenylacetyl moiety, a finding that was corroborated by the following ^1H and ^{13}C NMR signals: benzylic methylene δ_H 3.64 (2H, s, H-2′), δ_C 40.6; *p*-substituted aromatic ring δ_H 7.18 (2H, d, J_{AB} = 8.7 Hz, H-4′,8′), δ_H 6.84 (2H, d, J_{AB} = 8.7 Hz, H-5′,7′), and δ_C 158.7 (C-6′), 130.3 (C-4′,8′), 125.8 (C-3′), 114.0 (C-5′,7′); methoxy group δ_H 3.79 (3H, s, H-9′), δ_C 55.2 (Table 2). Compounds **1** and **2** are therefore ingol 7,8,12-triacetate 3-phenylacetate or 3-(4-methoxyphenyl)acetate, respectively.

Compound **3**'s molecular formula was established on the basis of HREIMS data from the *m/z* 582.2819 ion as $C_{33}H_{42}O_9$. Its NMR spectral data were very similar to those of **1**, differing only in the ester residue (Tables 1 and 2). In the ^1H and ^{13}C NMR spectra of **3**, the signals for one acetyl group were missing, while signals for an additional methyl group were present. Following the chemical shift assignment of all carbons and protons on the basis of the ^1H–^1H COSY, HSQC and HMBC spectra, it was concluded that **3** possesses a methoxy group on C-8 as is evident from the observed paramagnetic shift of the position 8 signals from δ_H 4.52 dd (1H, dd, *J* = 1.9, 10.7 Hz) and δ_C 71.4 in compound **1**, to δ_H 2.87 (1H, dd, *J* = 1.9, 10.1 Hz) and δ_C 78.4 in **3**. The relative configurations of the stereogenic centres of **3** were assigned following analysis of the NOESY spectrum (Table 3) and by comparing the chemical shifts and coupling constant of compounds **3** and **1**. Based on all of these evidences, the structure of compound **3** was established as 8-methoxyingol 7,12-diacetate 3-phenylacetate (**3**).

Compound **4** was isolated as a colourless powder, mp 181–182 °C, $[\alpha]_D^{20}$: +15° (*c* 2.3, $CHCl_3$). Its HREIMS spectrum showed a molecular ion peak at *m/z* 446.3759 (M^+), corresponding to the molecular formula $C_{29}H_{50}O_3$. The IR spectrum showed particular absorption for hydroxy (3472 cm^{-1}) and carbonyl groups (1692 cm^{-1}). The ^1H NMR spectrum revealed the presence of two methyl group doublets at δ_H 0.86 (3H-7″, d, *J* = 6.1 Hz), (3H-10, d, *J* = 6.7 Hz) and three methyl

Table 2. ^{13}C NMR[a] data of compounds **1**–**3** (150 MHz, δ [ppm])

C	1	2	3
1	31.4	31.4	31.4
2	29.5	29.5	29.3
3	76.8	76.7	77.2
4	73.4	73.3	73.3
5	117.1	117.1	117.0
6	139.2	139.3	139.6
7	76.9	76.8	74.6
8	71.4	71.4	78.4
9	24.6	24.6	26.8
10	19.2	19.2	19.3
11	29.4	30.6	30.5
12	70.6	70.6	71.1
13	43.0	43.0	42.8
14	207.5	207.5	207.6
15	71.1	71.1	71.1
16	16.9	16.9	16.9
17	17.4	17.4	17.6
18	29.1	29.1	29.2
19	16.0	16.0	16.2
20	13.4	13.4	13.4
OAc	20.5, 20.9, 21.0, 170.6, 170.9, 170.3	20.5, 20.9, 21.0, 170.3[b], 170.6[b], 170.7[b]	20.5, 21.1
			170.7[b], 170.6[b]
R_1	41.5, 133.8, 129.3, 128.6, 127.2, 170.2	55.2, 40.6	41.3, 134.0, 129.4, 128.5, 127.2, 170.5[b]
		114.0, 130.3 125.8, 158.7 170.2	
OMe			56.4

[a] Recorded in $CDCl_3$ (δ_C 77.0).
[b] Interchangeable signals.

group singlets at δ_H 1.16 (3H-10′, s), 1.44 (3H-11, s), 0.62 (3H-11′, s), one isopropyl group at δ_H 0.82 (3H-8″, d, J = 2.05 Hz), 0.83 (3H-6″, d, J = 2.05 Hz) and two hydroxymethine groups at δ_H 4.3 (H-8, dd, J_1 = 7.7 Hz, J_2 = 3.1 Hz), 3.0 (H-3, ddd, J_1 = 10.8 Hz, J_2 = 9.8 Hz, J_3 = 5.2 Hz). The ^{13}C NMR and DEPT spectra displayed signals corresponding to seven CH_3, 10 CH_2, seven CH [with two hydroxymethine groups at δ_C 77.2 (C-3) and δ_C 80.4 (C-7)] and five quaternary carbons [with one carbonyl group at δ_C 215.0 (C-8)]. Comparison of these spectral data with those of 4α,14α-dimethyl-5α-cholest-8-en-3β-ol (**5**); 3β,7α-dihydroxy-4α,14α-dimethyl-5α-cholest-8-en-11-one and 3β,7β-dihydroxy-4α,14α-dimethyl-5α-cholest-8-en-11-one, previously isolated from *E. officinarum* by our research group,[24,25] suggests that the skeletons of the A and D rings (including the side-chain moiety) were quite similar. This conclusion was supported by extensive study of the HMBC spectrum which exhibited the following cross-peak correlations: H-18/C-12, C-13, C-14, C-17; H-21/C-17, C-20, C-22; H-32/C-13, C-14, C-15; H-30/C-3, C-4, C-5 and H-19/ C-1, C-9, C-10. Furthermore, the allocation of the quaternary C-8 and oxymethine carbons C-7 was confirmed by the correlation of H-7 with C-5 and C-11; H-19 with C-9 and H-32 with C-8. The structure and stereochemistry of **4** were further confirmed by means of X-ray single-crystal crystallography analysis (Fig. 2).

The fact that **4** and **5** coexist in the same plant leads us to suggest a reasonably plausible biosynthetic pathway for compound **4** (Scheme 2). Thus, allylic oxidation[26,27] followed by epoxidation gives the hydroxyepoxide which then rearranges to spiroterpenoid (**4**). A similar mechanism has been proposed by other research groups investigating the triterpenic components of *Euphorbia supina* and *Ficus microcarpa*.[28,29]

The cell cycle is a complex, specific sequence of events that directs the growth and proliferation of cells. Cell cycle events are divided into four phases designated as G_0/G_1, S, G_2 and M, and the major molecular players in cell-cycle progression are the cyclin-dependent kinases (CDKs) and their regulatory counterparts, the cyclins. Control of cell-cycle progression is achieved by a periodic, sequential expression and degradation of cyclins which bind to, and transiently activate, their respective CDKs.[30] Since other *Euphorbia*-derived natural com-

Table 3. NOESY and HMBC correlations of compounds **1**–**3**

	1		2		3	
	^1H-^1H NOESY	HMBC	^1H-^1H NOESY	HMBC	^1H-^1H NOESY	HMBC
H-1α,	H1β, H2	C2, C15, C16	H1β, H2	C2, C15, C16	H1β, H2	C2, C15, C16
H-1β,	H1α, H16	C2,C3, C4, C16	H1α, H16	C2, C3, C4, C15, C16	H1α, H16	C2, C3, C4, C15, C16
H-2	H16, H_21	C4, C15, C16	H1α, H3, H16	C4, C15, C16	H1α, H3, H16	C4, C15, C16
H-3	H2, H5	C1, C15	H2, H5	C2, C16	H2, H5	C2, C16
H-5	H3,H9	C4, C6, C7, C3	H3,H9	C3, C4, C6, C7, C17	H3,H9	C4, C6, C17
H-7	H8, $COCH_3$	C5, C6 ,C9, C17, $COCH_3$	H8, $COCH_3$	C5, C6, C8,C9, C17,	H8, $COCH_3$, OCH_3	C5, C6,C9, C17,
H-8	H7, H12, H13, H19, $COCH_3$	C9, $COCH_3$	H7, H12, H13, H19, $COCH_3$	C7, C9, C11, $COCH_3$	H7, H12, H17,	C7, C9,
H-9	—	C7, C18	H5, H18	C7, C8,C18	H5,	—
H-11	—	C8, C9, C13	—	—	—	—
H-12	H8, H13, H18, H19	C11, C14, $COCH_3$	H8, H13, H19	C14	H8, H13, H19	C11, C14,
H-13	H12, H8, H20	C14	H12, H20	C14, C20	H12, H20	C14, C20
H-16	H2, H1β	C1, C3	H2, H1 β	C1, C2, C3	H2, H1β	C1,C2, C3
H-17	H3	C5, C6, C7	—	C5, C6	H7,H8	C5, C6, C7
H-18	H12	C9, C10, C11, C19	—	C9, C10, C11, C19	H9	C10, C-19
H-19	H12, H8, H18	C9, C10, C11, C18	H8, H12, H18	C9, C10, C11, C18	H8, H12, OCH_3	C9, C10, C11, C19
H-20	—	C12, C14	—	C12, C13, C14	H13	C12, C13, C14

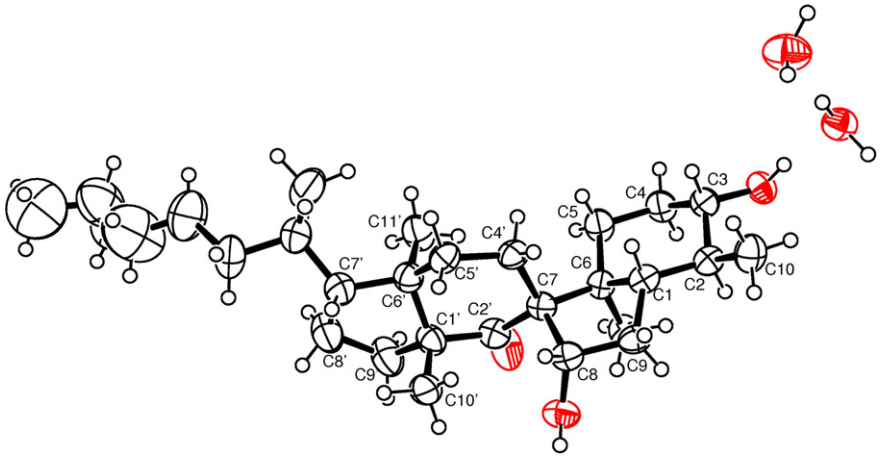

Figure 2. ORTEP drawing of **4**.

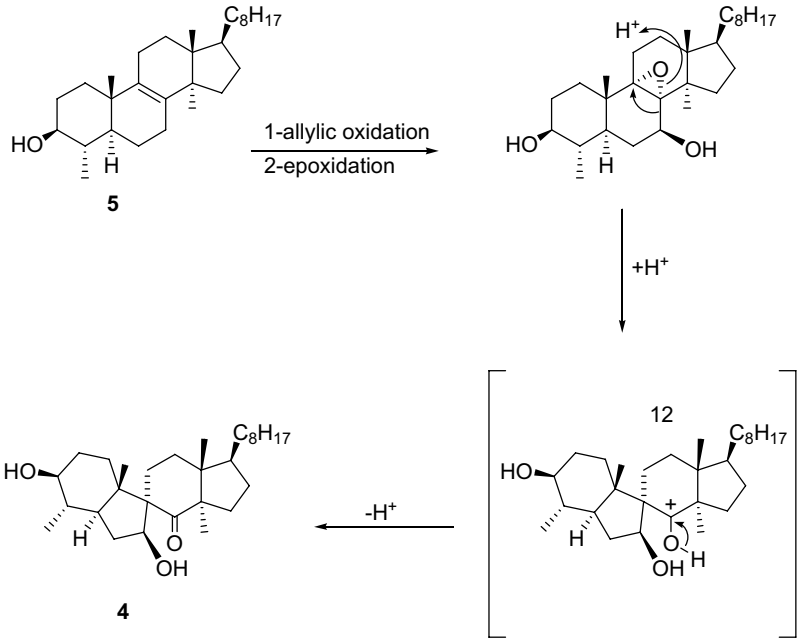

Scheme 2. Proposed mechanism for the biogenesis of **4**.

pounds have been shown to interfere with cell-cycle progression in cancer cells,[8–10] we investigated the effects of compounds **1**–**3** on the different phases of the cell cycle in Jurkat-LTR-GFP cells. To this end, the cells were treated with 10 or 50 μM of each compound for 36 h and compared to untreated control cells which were fully cycling and progressed through the S, G2 and M phases of the cell cycle (34% of the cells). However, and while compounds **1** and **2** did not affect cell cycle, compound **3**-treated cells showed a clear decrease in the percentage of cells in the S and G_2/M phases, correlating with an increase in the percentage of cells at the G_0/G_1 phase (Table 4). Thus, at the concentrations tested, we observed that compound **3** is not cytotoxic on its own but rather prevents cell proliferation by arresting the cells at the G_0/G_1 phase of the cell cycle. These results encouraged us to study the activity of compound **3** on HIV-LTR transactivation by measuring the levels of GFP as a marker of HIV promoter activation. As depicted in Fig. 3, this compound was able to activate the HIV-LTR promoter in a concentration-dependent manner. Interestingly, compounds **1** and **2** did not show any effect on HIV-LTR transactivation (data not shown). Our whole set of results suggests that compound **3** may target a common signalling pathway resulting in both G_o/G_1 cell-cycle arrest and HIV-1-LTR promoter activation and is therefore a novel lead compound for the development of therapies against HIV-1 latency.

3. Experimental

3.1. Plant material

Latex from *E. officinarum* was collected in April, 2003, from plants on the North Atlantic coast of Agadir, Morocco. Latex was obtained by making repeated cuts along

Table 4. Effects of compounds on cell cycle phases in Jurkat-LTR-GFP cells[a]

	Sub-G_0 (%)	G_0/G_1 (%)	S (%)	G_2/M (%)
Control	1.16	64.6	18.3	15.7
1 (10 μM)	1.52	61.5	20.9	15.9
1 (50 μM)	1.38	66.2	18.7	13.4
2 (10 μM)	1.59	60.9	21	16.4
2 (50 μM)	1.95	61.5	21.7	14.7
3 (10 μM)	2.34	77.8	9.01	10.8
3 (50 μM)	3.97	81.4	5.31	9.22

[a] Jurkat-LTR-GFP cells were incubated with **1**–**3** at the indicated concentrations for 36 h. DNA was stained and cells analysed by flow cytometry. The percentages of cells in the different phases of the cell cycle were calculated using Cylchred V.1.0.2 cell-cycle analysis software.

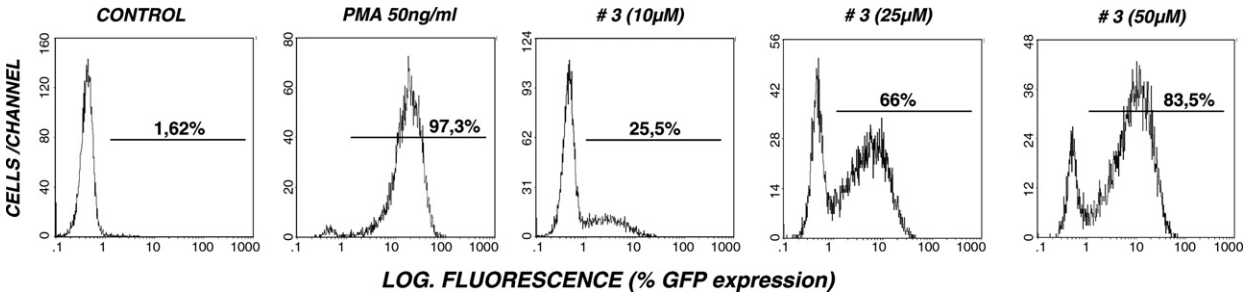

Figure 3. Effects of compound **3** on HIV-LTR-dependent GFP expression.

the stems of the plants with a knife and collecting the white milky exudates. A voucher specimen is on deposit at the herbarium of the Chemistry Laboratory of Natural Substances, University Cadi Ayyad.

4. Materials and methods

The latex (0.5 L) from *E. officinarum* was allowed to dry and the resulting coagulum (200 g) was extracted with MeOH (1.5 L) in a Sohxlet apparatus. The MeOH solution was cooled to yield a precipitate (60 g), which was then subjected to silica gel column chromatography. Elution of the column with hexane:ethyl acetate (95:5) afforded three fractions [fraction (weight after solvent removal)]: A (5 mg), B (4 g) and C (53 g) while elution with hexane:ethyl acetate (90:10) gave a fourth fraction D (16 mg). Analysis of fractions A–C by means of chromatography on silica gel 10% $AgNO_3$ yielded known compounds.[21] Further analysis of fraction C on a silica gel column with hexane: acetone (95:5) yielded 7,8,12-triacetyl-3-phenylacetylingol (**1**) (4 mg); 7,8,12-triacetyl-3-(4-methoxyphenyl)acetylingol (**2**) (9 mg) and 7, 12-diacetyl-8-methoxy-3-phenylacetyl-ingol (**3**) (5 mg). Purification of fraction D by means of HPLC with hexane:ethyl acetate (72:28) yielded known compounds[24,25] along with the spirotriterpene (**4**) (5 mg). The spectral data of the new compounds are given below.

5. General experimental procedures

Optical rotations were determined with a Perkin-Elmer 241 polarimeter. IR spectra were recorded on a Mattson Genesis spectrophotometer, series FTIR (Fourier-transform infrared). ^1H and ^{13}C NMR spectra and 2D NMR spectra were recorded on Varian Unity 400 and 600 NMR spectrometers with $SiMe_4$ as the internal reference. Mass spectra were recorded on Fisons MD800 and Finnigan MAT95 S instruments. HPLC was performed with a Hitachi/Merck L-6270 apparatus equipped with an UV/vis detector (L 4250) and a differential refractometer detector (RI-71). Thin-layer chromatography (TLC) was performed on Merck Kieselgel 60 F254, 0.2 mm thick (Catalog No. 1.05554.0001). Silica gel (Merck) was used for column chromatography. All solvents used were freshly distilled.

5.1. Ingol 7,8,12-triacetate 3-phenylacetate (1)

Amorphous solid, $[\alpha]_D^{20}$: +5.28 °(*c* 0.21, $CHCl_3$); IR (film) ν_{max} 1760, 1720, 1578, 712 cm^{-1}; ^1H and ^{13}C NMR, Tables 1–3. EIMS (*m*/*z*) 610 (7 %) [$M^{+\cdot}$], 312 (7%), 284 (6%), 245 (7%), 192 (8%), 181 (11%), 165 (12%), 163 (11%), 138 (15%), 122 (15%), 105 (32%), 91 (100%), 43 (46%), HREIMS (*m*/*z*) 610.2800, calcd. for $C_{34}H_{42}O_{10}$, 610.2778 (mass error + 0.0022).

5.2. Ingol 7,8,12-triacetate 3-(4-methoxyphenyl)acetate (2)

Amorphous solid, $[\alpha]_D^{20}$: −9.15 ° (*c* 0.47, $CHCl_3$); IR (film) ν_{max} 1736, 1704 cm^{-1}; ^1H and ^{13}C NMR, Tables 1–3. EIMS (*m*/*z*) 610 (2 %) [$M^{+\cdot}$], 148 (19%), 121 (100%), 43 (16%), HREIMS (*m*/*z*) 640.2874, calcd. for $C_{35}H_{44}O_{11}$, 640.2883 (mass error − 0.0009).

5.3. 8-Methoxyingol 7,12-diacetate 3-phenylacetate (3)

Amorphous solid, $[\alpha]_D^{20}$: −2.61 ° (*c* 0.34, $CHCl_3$); IR (film) ν_{max} 1731, 1707 cm^{-1}; ^1H and ^{13}C NMR, Tables 1–3. EIMS (*m*/*z*) 582 (37 %) [$M^{+\cdot}$], 111 (32%), 91

(100%), 43 (30%), HREIMS (*m*/*z*) 582,2819, calcd. for $C_{33}H_{42}O_9$, 582.2828 (mass error −0.0009).

5.4. 3*S*,4*S*,5*R*,7*S*,9*R*,14*R*-3,7-Dihydroxy-4,14-dimethyl-7[8 → 9]-*abeo*-cholestan-8-one (4)

Colourless crystals, mp 181–182 °C; $[\alpha]_D^{20}$: +15 ° (*c* 2.3, $CHCl_3$); IR (film): ν_{max} 3472, 1691 cm^{-1}; ^1H NMR ($CDCl_3$, 400 MHz) δ (ppm): 4.3 (H-7, dd, J_1 = 7.7 Hz, J_2 = 3.1 Hz), 3.0 (H-3, ddd, J_1 = 10.8 Hz, J_2 = 9.8 Hz, J_3 = 5.2 Hz), 2.33 (H-6β, ddd, J_1 = 13.3 Hz, J_2 = 7.7 Hz, J_3 = 6.6 Hz), 1.16 (H_3-32, s), 1.44 (H-19, s), 0.91 (H_3-30, d, J = 6.7 Hz), 0.62 (H_3-8, s), 0.86 (H_3-21, d, J = 6.1 Hz), 0.82 (H_3-26, d, J = 2.05 Hz), 0.83 (H_3-24, d, J = 2.05 Hz).^{13}C NMR (100 MHz, $CDCl_3$) δ (ppm): 28.7 (t, C-11), 215.0 (s, C-8), 64.0 (s, C-9), 77.2 (d, C-3), 80.4 (d, C-7), 30.1 (t, C-12), 61.0 (s, C-14), 50.2 (d, C-17), 47.6 (s, C-13), 48.1 (d, C-5), 39.4 (t, C-11), 48.0 (s, C-10), 38.1 (d, C-4), 35.6 (d, C-20), 36.1 (t, C-22), 29.5 (t, C-1), 31.1 (t, C-2), 30.7 (t, C-15), 37.7 (t, C-6), 27.9 (d, C-25), 22.7 (t, C-16), 19.7 (q, C-32), 24.0 (t, C-23), 22.7 (q, C-27), 22.5 (q, C-26), 18.7 (q, C-21), 18.3 (q, C-19), 16.2 (q, C-18), 16.1 (q, C-30). HMBC: (H-7/C-5, C-11); (H_3-18/C-12, C-13, C-14, C-17); (H_3-19/C-1, C-9, C-10); (H_3-21/C-17, C-20, C-22); (H_3-10/C-3, C-4, C-5); (H_3-10/C-8, C-13, C-15, C-14). EIMS(m/z) 446 (19%) [M^+], 428 (35%) [M^+-18], 413 (10%) [M^+-18−Me], 371 (21%), 329 (24%), 307 (45%), 301 (20%), 207 (47%), 177 (19%), 165 (41%), 149 (20%), 122 (28%), 109 (39%), 108 (14%), 107 (40%) , 165 (43%), 95 (100%). MS (*m*/*z*) 446.3755, calcd. for $C_{29}H_{50}O_3$, 446.3759 (mass error − 0.0004).

5.5. Crystal data and structure determination of compound 4

$C_{29}H_{54}O_5$ (co-crystallized with two H_2O molecules), *M*r 482.72, monoclinic, space group $P2_1$, a = 10.4710(3) Å, b = 6.4805(2) Å, c = 21.2682(8) Å, β = 94.797(1)°, V = 1438.25(8) $Å^3$, Z = 2, Dc = 1.115 mg m^{-3}, $F(000)$ = 536, λ = 0.71073 Å, μ = 0.078 mm^{-1}. Data were collected from a $0.30 \times 0.15 \times 0.10$-$mm^3$ crystal on a Bruker–Nonius KappaCCD diffractometer.[31] Temperature 293(2) K. A total of 10,178 reflections were collected for $1.92 < \theta < 25.99°$ and $-12 \leqslant h \leqslant 12$, $-7 \leqslant k \leqslant 7$, $-26 \leqslant l \leqslant 26$. There were 3039 independent reflections. There was no crystal decay and no absorption correction was applied. The structure was solved by means of direct methods with SIR92[32] and refined with SHELXL-97[33] to final indices $R[F^2 > 4\sigma F^2]$: 2521 reflections] = 0.0682 and wR [all reflections] = 0.1745, [$w = 1/[\sigma^2(Fo^2) + (0.1346P)^2 + 6.2747P]$, where $P = (Fo^2 + 2Fc^2)/3$]. The hydrogen atoms were placed in calculated positions and added to the refinement as a fixed isotropic contribution. The goodness-of-fit on F^2 was 1.041; the last residual Fourier-positive and -negative peaks were equal to 0.251 and −0.297, respectively.

5.5.1. Biological assays

5.5.1.1. Determination of HIV-1-LTR promoter transcription. Jurkat-LTR-GFP is a Jurkat-derived clone latently infected with a recombinant virus containing the GFP gene driven by the HIV-LTR promoter and its full characterization will be described elsewhere. The cells were stimulated with either phorbol 12-myristate 13-acetate (PMA) or compound **3** for 36 h and the GFP expression was analysed by flow cytometry in an EPIC XL flow cytometer (Coulter, Hialeah, FL). Ten thousand gated events were collected per sample and the fluorescence pattern was determined.

5.5.1.2. Cytofluorimetric analyses of cell cycle. Cells (10^6) were treated with compounds **1**–**3** for 36 h. After treatment, cell-cycle analysis was performed by fixing the cells in ethanol (70% for 24 h at 4 °C) followed by RNA digestion (RNAase 50 U/mL) and DNA staining with propidium iodide (PI) (20 μg/ml) for 2 h prior to cytometric analysis. Ten thousand gated events were collected per sample, and the percentage of cells in each phase of the cell cycle was calculated using Cylchred V.1.0.2 cell-cycle analysis software (University of Wales College of Medicine, Cardiff, UK).

Acknowledgment

This work was supported in part by the Alfa Programme of the European Community; EULADIV Project (AML/B7-311/97/0666/II-0375-FA). We thank Dr. Michel Giorgi from the University of Marseille III for the generous x-Ray analysis.

References and notes

1. Tian-Shung, W.; Yuh-Meei, L.; Haruna, M. *J. Nat. Prod.* **1991**, *54*, 823.
2. Ferrigni, N. R.; McLaughlin, J. L.; Powell, R. G.; Smith, C. R. *J. Nat. Prod.* **1984**, *47*, 347.
3. Hartwell, J. L. *J. Nat. Prod.* **1969**, *32*, 153.
4. Fatope, M. O.; Zeng, L.; Ohayaga, J. E.; Shi, G.; McLaughlin, J. L. *J. Med. Chem.* **1996**, *39*, 1005.
5. Kupchan, S. M.; Uchida, I.; Branfman, A. R.; Dailey, R. G.; Fei, B. Y. *Science* **1976**, *191*, 571.
6. Hecker, E. P. *Appl. Chem.* **1977**, *49*, 1423.
7. Appendino, G.; Szallasi, A. . *Life Sci.* **1999**, *60*, 681.
8. Irie, K.; Nakahara, A.; Nakagawa, Y.; Ohigashi, H.; Shindo, M.; Fukuda, H.; Konishi, H.; Kikkawa, U.; Kashiwagi, K.; Saito, N. . *Pharmacol. Ther.* **2002**, *93*, 271.
9. Kedei, N.; Lundberg, D. J.; Toth, A.; Welburn, P.; Garfield, SH.; Blumberg, P. M. *Cancer Res.* **2004**, *64*, 3243.
10. Ma, D. *Curr. Med. Chem.* **2001**, *8*(2), 191.
11. Hezareh, M. *Drug News Perspect.* **2005**, *8*, 496.
12. Szallasi, Z.; Blumberg, P. M. *Cancer Res.* **1991**, *51*(19), 5355.
13. Kulkosky, J.; Culnan, D. M.; Roman, J.; Dornadula, G.; Schnell, M.; Boyd, M. R.; Pomerantz, R. J. *Blood* **2001**, *98*, 3006.
14. Sierra, S.; Kupfer, B.; Kaiser, R. B. *J. Clin. Virol.* **2005**, *34*, 233.
15. Lotter, H.; Opferkuch, H. J.; Hecker, E. *Tetrahedron Lett.* **1979**, *20*, 77.
16. Ravikanth, V.; Reddy, V. L. N.; Reddy, A. V.; Ravinder, K.; Rao, T. P.; Ram, T. S.; Kumar, K. A.; Vamanarao, D. P.; Venkateswarlu, Y. *Chem. Pharm. Bull.* **2003**, *51*, 431.
17. Marco, J. A.; Sanz Cervera, J. F.; Ropero, F. J.; Checa, J.; Fraga, B. M. *Phytochemistry* **1998**, *49*, 1095.

18. Ravikanth, V.; Reddy, V. L. N.; Rao, T. P.; Diwan, P. V.; Ramakrishna, S.; Venkateswarlu, Y. *Biochem. Syst. Ecol.* **2003**, *31*, 447.
19. Hergenhahn, M.; Kusumoto, S.; Hecher, E. *Experientia* **1974**, *30*, 1438.
20. Morgenstern, T.; Bittner, M.; Silva, M.; Aqueveque, P.; Jakupovic, J. *Phytochemistry* **1996**, *41*, 1149.
21. Marco, J. A.; Sanz Cervera, J. F.; Yuste, A. *Phytochemistry* **1997**, *45*, 563.
22. Evans, F. J.; Taylor, S. E. *Prog. Chem. Org. Nat. Prod.* **1983**, *44*, 1.
23. Stewart, J. J. P. *J. Comput. Chem.* **1989**, *10*, 209, 221.
24. Benharref, A.; Lavergne, J. P. *Bull. Soc. Chim. Fr.* **1985**, *5*, 852.
25. Daoubi, M.; Benharref, A.; Hernández-Galán, R.; Macías-Sánchez, A. J.; Collado, I. G. *Nat. Prod. Res.* **2004**, *18*, 177.
26. Wuest, Matthias; Beck, Thomas; Mosandl, Armin *J. Agric. Food Chem.* **1998**, *46*, 3225.
27. Shirane, Noboru; Sui, Zhihua; Peterson, Julian A.; Ortiz de Montellano, Paul R. *Biochemistry* **1993**, *32*, 13732.
28. Tanaka, R.; Matsunaga, S. *J. Pharm. Soc. Jap.* **1999**, *119*, 319.
29. Chiang, Y. M.; Kuo, Y. H. *J. Org. Chem.* **2002**, *67*, 7656.
30. Johnson, D. G.; Walker, C. L. *Ann. Rev. Pharmacol. Toxicol.* **1999**, *39*, 295.
31. Bruker-Nonius. Kappa CCD Reference Manual; Nonius B.V., PO Box 811, 2600 Av., Delft, The Netherlands; **1998**.
32. Altamore, A.; Cascarano, G.; Giacovazzo, C.; Guagliardi, A.; Burla, M. C.; Polidori, G.; Camalli, M. *J. Appl. Cryst.* **1994**, *27*, 435.
33. Sheldrick, G. M. *SHELXS-97, Program for the Solution of Crystal Structures*; University of Gottingen: Gottingen, Germany, 1997.